ARMY RESEARCH LABORATORY

Scanning Tunneling Microscopic Characterization of an Engineered Organic Molecule

by Govind Mallick, Pamela Kaste, and Shashi P. Karna

ARL-TR-5639 **August 2011**

NOTICES

Disclaimers

The findings in this report are not to be construed as an official Department of the Army position unless so designated by other authorized documents.

Citation of manufacturer's or trade names does not constitute an official endorsement or approval of the use thereof.

Destroy this report when it is no longer needed. Do not return it to the originator.

Army Research Laboratory
Aberdeen Proving Ground MD 21005-5069

ARL-TR-5639 **August 2011**

Scanning Tunneling Microscopic Characterization of an Engineered Organic Molecule

Govind Mallick
Vehicle Technology Directorate, ARL

Pamela Kaste and Shashi P. Karna
Weapons and Materials Research Directorate, ARL

REPORT DOCUMENTATION PAGE	Form Approved OMB No. 0704-0188

PLEASE DO NOT RETURN YOUR FORM TO THE ABOVE ADDRESS.

1. REPORT DATE *(DD-MM-YYYY)*	2. REPORT TYPE	3. DATES COVERED (From - To)
August 2011		01 January to 30April 2011

4. TITLE AND SUBTITLE	5a. CONTRACT NUMBER
Scanning Tunneling Microscopic Characterization of an Engineered Organic Molecule	5b. GRANT NUMBER
	5c. PROGRAM ELEMENT NUMBER
6. AUTHOR(S)	5d. PROJECT NUMBER
Govind Mallick, Pamela Kaste, and Shashi P. Karna	5e. TASK NUMBER
	5f. WORK UNIT NUMBER
7. PERFORMING ORGANIZATION NAME(S) AND ADDRESS(ES)	8. PERFORMING ORGANIZATION REPORT NUMBER
U.S. Army Research Laboratory ATTN: RDRL-VT Aberdeen Proving Ground MD 21005-5069	ARL-TR-5639
9. SPONSORING/MONITORING AGENCY NAME(S) AND ADDRESS(ES)	10. SPONSOR/MONITOR'S ACRONYM(S)
	11. SPONSOR/MONITOR'S REPORT NUMBER(S)

12. DISTRIBUTION/AVAILABILITY STATEMENT

Approved for public release; distribution unlimited.

13. SUPPLEMENTARY NOTES

14. ABSTRACT

Surface topology and electron transport properties of self-assembled monolayer (SAM) of an engineered molecule 4,4'-[1,4-phenylenebis(methylidynenitrilo)]bisbenzenethiol (PMNBT) and 1-dodecanethiol (dDT) adsorbed on Au substrates have been investigated by scanning tunneling microscopy (STM) at ambient conditions. The electrical measurements of hexadecanethiol (hDT), which is similar in length to PMNBT, have also been compared. The π-bond dominated PMNBT molecule was engineered using first-principle ab initio molecular orbital theory. The estimated conductance, $(dI/dV)_{v=0.75}$ = 123.91nS for PMNBT, is over an order of magnitude larger than the corresponding value (7.15nS) for dDT and two orders of magnitude larger (0.078nS) than hDT. The tunneling current (*I*) as a function of the applied bias (*V*) between STM tip and SAM of PMNBT exhibits asymmetric behavior. A combination of electronic and geometrical effects in the molecule and at the molecule-metal interface is proposed to be responsible for the observed asymmetric *I-V* characteristics. The increased conductance in PMNBT is also explained in terms of its nearest available electronic states.

15. SUBJECT TERMS

PMNBT, AFM, STM, hDT, dDT, SAM

16. SECURITY CLASSIFICATION OF:			17. LIMITATION OF ABSTRACT	18. NUMBER OF PAGES	19a. NAME OF RESPONSIBLE PERSON
a. REPORT	b. ABSTRACT	c. THIS PAGE	UU	22	Govind Mallick
Unclassified	Unclassified	Unclassified			19b. TELEPHONE NUMBER (*Include area code*) (410) 306-4735

Standard Form 298 (Rev. 8/98)
Prescribed by ANSI Std. Z39.18

Contents

List of Figures

List of Tables

Acknowledgment

This research was supported by the U.S. Army Research Laboratory (ARL) Director's Research Initiative (DRI), the Defense Advanced Research Projects Agency (DARPA)-MoleApps program, and the Air Force Office of Scientific Research-Defense University Research Initiative in Nanotechnology. Shashi P. Karna thanks Professor Paras Prasad and Dr. Qingdong Zheng for valuable discussions, and suggestions and their contributions of phenylenebis(methylidynenitrilo)]bisbenzenethiol (PMNBT) molecules. Shashi P. Karna and Govind Mallick thank Raymond Woo and Ravi Pandey for valuable discussions and suggestions, and Sarah Lastella and Anubhav Srivastava for their valuable contributions.

INTENTIONALLY LEFT BLANK.

1. Introduction and Background

Rectification of electrical current between two metal electrodes by suitably engineered organic molecules was first proposed by Aviram and Ratner (*1*), who showed from semi-classical theoretical calculations that an organic molecule with π(donor)-σ(spacer)-π(accepter) architecture, sandwiched between two metal electrodes, would allow electrons to tunnel only from the donor to the acceptor side of the molecule. The Aviram-Ratner model has since been verified in several experimental (*2–7*) and theoretical investigations (*7, 8*) involving suitably engineered donor (D)–acceptor (A) substituted organic molecules. Recently, there have also been reports of rectification behavior by molecules that do not contain D–A architectures, but are assembled between dissimilar metal contacts. When probed by scanning tunneling microscopy (STM), copper-4,4',4",4'"-tetraaza-29H,31H-phthalocyanine molecules adsorbed on graphite (*9*), 3,10-didocecylperylene also adsorbed on graphite (*10*), and oligo(phenylene ethynylene) molecules adsorbed on gold (Au)(111) and silver (Ag)(111) substrates (*11*) have been shown to exhibit rectification of tunnel current. Rectification by oligo(phenylene ethynylene) molecules adsorbed between Au cross-wire junctions (*12*) and chemical vapor-deposited (CVD) single wall carbon nanotubes (SWCNTs), previously thought to be symmetric structures, have also been recently reported (*13*, *14*).

We report the STM observation of rectification by a newly designed and synthesized 4,4'-[1,4-phenylenebis(methylidynenitrilo)]bisbenzenethiol (PMNBT) molecule adsorbed on thin film Au substrate. Alkanethiol molecules [$CH_3(CH_2)_{n-1}SH$] form a robust self-assembled monolayer (SAM) on Au surfaces and are studied explicitly. STM (*15*) and conducting atomic force microscopy (cAFM) (*16*) have been used to study the electron transport (ET) through alkanethiols at room temperature. In this study, we have designed and modeled the PMNBT molecule using first principle *ab initio* methods. The ET properties of the SAM of the synthesized PMNBT molecule, along with the SAMs of hexadecanethiol (hDT) and dodecanethiol (dDT) on a thin film Au substrate, were measured using STM at ambient conditions. Although similar in size, because PMNBT is a π-bonded molecule and hDT is not, the current (*I*)–voltage (*V*) characteristics are different, as would be expected. Tunnel current through PMNBT molecules exhibits almost twice as much asymmetric *I–V* characteristic as the hDT and dDT molecules. We attribute the observed rectification by the PMNBT molecule to its highly delocalized π-electron in the highest occupied molecular orbital (HOMO) and electron-rich (Donor) characteristics of the S atom chemisorbed on Au surface.

2. Materials and Methods

Theoretical calculations were performed using an ab initio Hartree-Fock (HF)-based effective core potential (ECP), with a CEP-121G minimal basis set to obtain the equilibrium structure of the Au-PMNBT-Au (Au-S-C_6H_4-N=CH-C_6H_4-CH=N-C_6H_4-S-Au) molecule. The optimized structure, along with its corresponding HOMO and lowest unoccupied molecular orbital (LUMO), are shown in figure 1. The overall length (R_{Au-Au}) of the molecule was computed to be 2.16 nm.

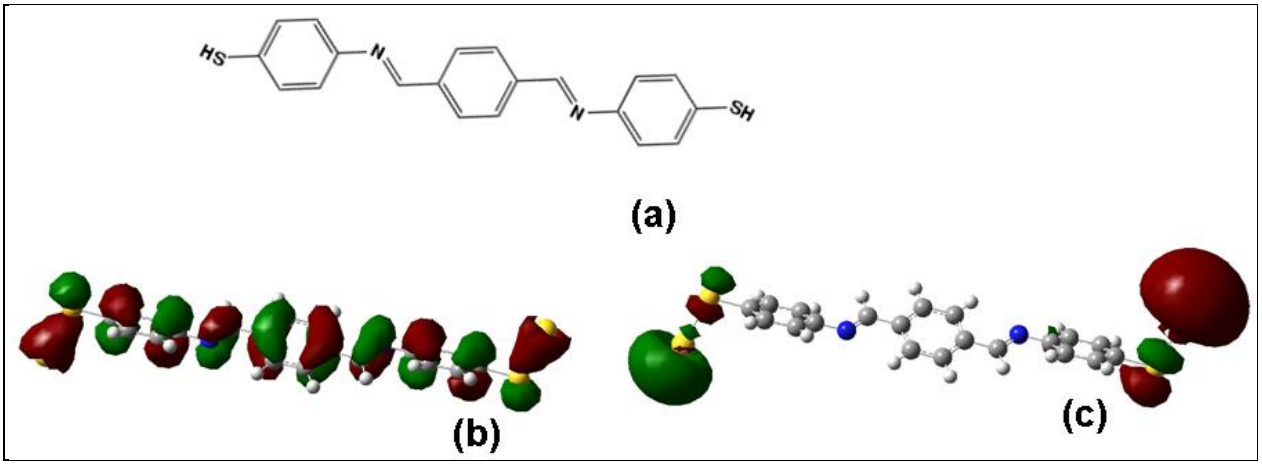

Figure 1. Stick model of the PMNBT molecule (a), and its highly occupied molecular orbitals (HOMO) (b), and lowest unoccupied molecular orbitals (LUMO) (c); $\Delta\varepsilon$ (HOMO-LUMO) = 7.0343 eV. The N-C-C_6H_4-C-N moiety of the optimized molecule is out of plane by 32.88^o indicating the asymmetric nature of the molecule (1c).

The PMNBT molecule was synthesized (*17*) by condensation between two equivalents of 4-aminothiophenol and one equivalent of 1,4-benzenedicarboxaldehyde, with a yield of 85%. The molecular structure of the compound, shown in figure 1a, was confirmed by ^{1}H NMR, ^{13}C NMR, and elemental analyses. The absorption maximum (λ_{max}) and the extinction coefficient of PMNBT in THF are 315 nm and $1.2 \times 10^4\ M^{-1}cm^{-1}$, respectively. The commercially available Au substrate (Molecular Imaging, Tempe, AZ) with an average roughness of ~0.3 nm was used as the surface upon which the SAMs of PMNBT, hDT, and dDT were deposited. The Au substrate as obtained was first treated with UV/Ozone to remove any assortment of organic contaminants from the surface. For the preparation of the hDT and dDT SAMs, the Au substrate was separately incubated in a 1 mM ethanol solution of 1-hexadecanethiol (Acros Organics, 92%) and 1-dodecanethiol (Aldrich, 98%) for an overnight period of more than 12 h. Subsequently, the film was rinsed with ethanol and dried in air. A 1.13×10^{-3} M solution of PMNBT (molecular weight = 348 g/mol) was prepared in tetrahydrofuran (THF). The SAMs of PMNBT were prepared by incubating a clean Au (mentioned previously) substrate in the THF

solution. The substrate was rinsed with THF and air-dried. The surface topologies of the bare and molecule adsorbed substrates were characterized by STM conductance spectroscopy (CP-II, Veeco Inc.), as shown in the schematic diagram in figure 2a. The STM topologies (figures 2b (dDT) and 2c (PMNBT)) and respective height profiles (figures 2d and 2e) allowed the identification of the regions on the substrate surface with bundles of adsorbed molecules (hDT– not shown).

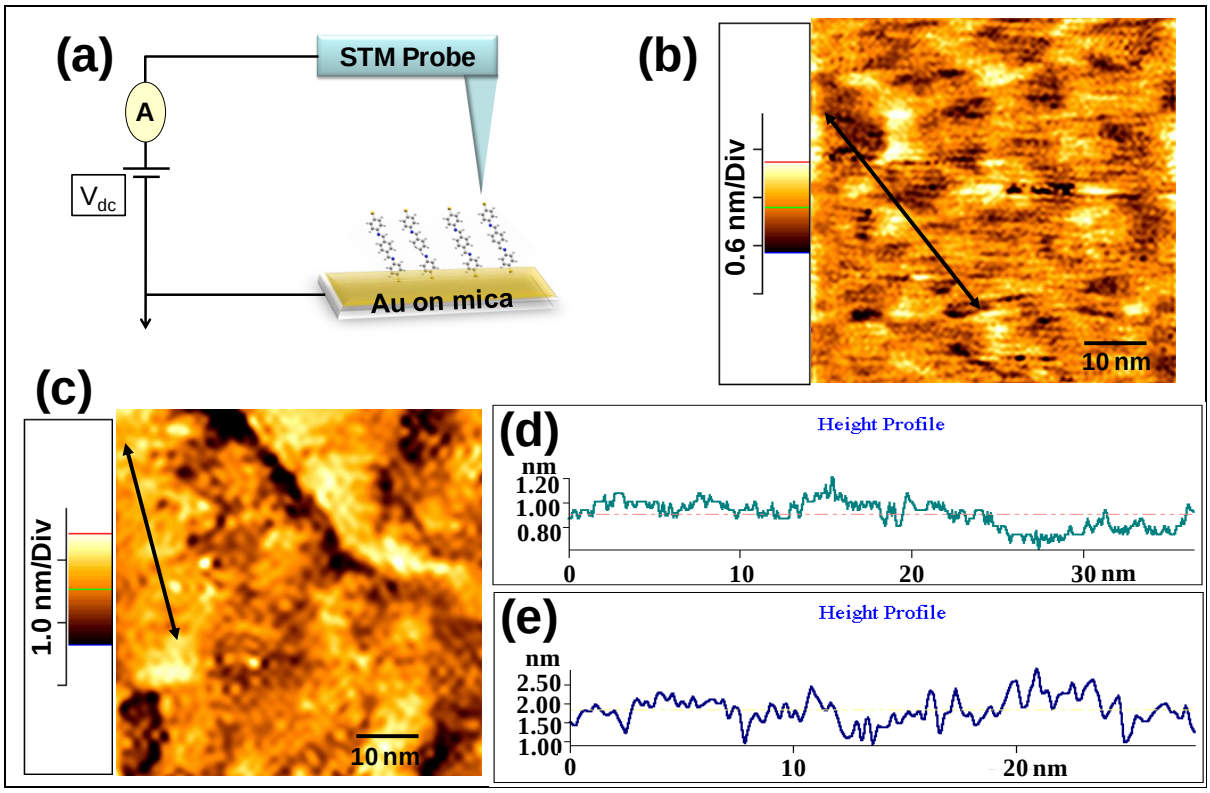

Figure 2. Schematic diagram of proposed STM characterization (a). STM topographical image of 50 x 50 nm^2 scan area showing SAM of dDT (b) and PMNBT (c) molecules on Au surface. The height profiles shown in (d) and (e) indicate average lengths of 1.2 and 2.1 nm of dDT and PMNBT, respectively.

For further verification of molecules on the Au substrates, Fourier Transform Infrared (FTIR) spectroscopy was performed. A Thermo Nicolet Nexus 870 FTIR, with a grazing angle attachment and wide-band MCT detector, was used. Figure 3 shows the spectra obtained for SAM of PMNBT (top), which was compared to raw crystal PMNBT molecules (bottom).

The STM *I–V* measurements were then performed at clearly marked areas of SAMs of PMNBT (figure 4a), hDT (figure 4b), and dDT (figure 4c), respectively. In the STM measurements, freshly cut platinum/iridium (Pt/Ir) tips were used for each sample. The tip was lowered to the sample for a set tunnel current of 2 nA at a tip-to-sample bias of 0.13 V. In the *I–V* trace, data taken at the same points for over 100 traces were averaged in order to reduce random noise, especially in the high bias region. Figure 4d shows the average second-order STM *I-V* curves of each molecule.

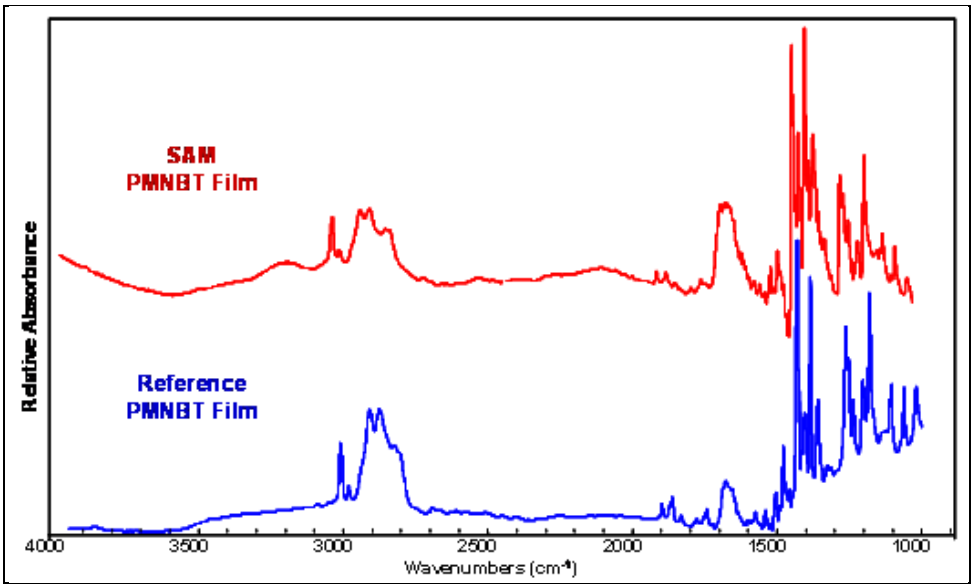

Figure 3. The grazing angle FTIR spectra of a reference sample of PMNBT crystals (bottom), and a SAM film of PMNBT (top) molecules on the Au surface.

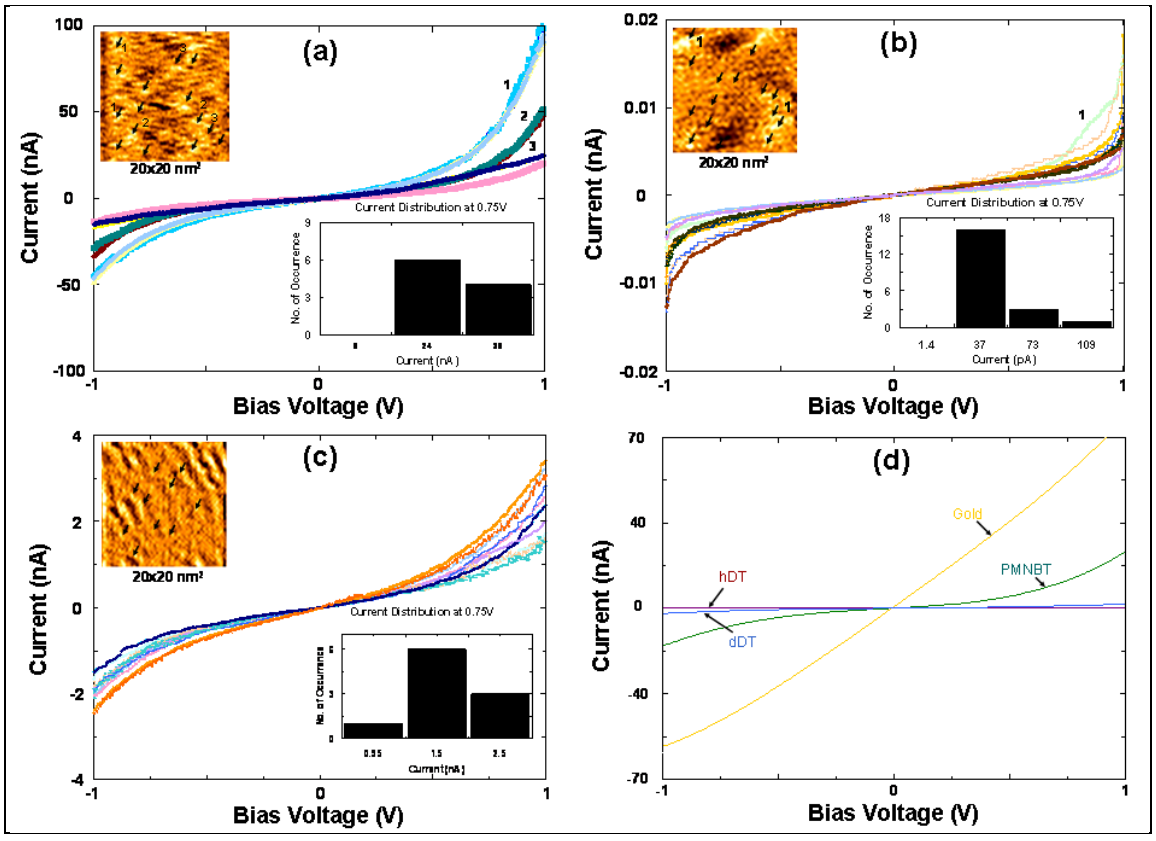

Figure 4. The current (*I*) as a function of bias voltage (*V*) at set point tunneling current and sample bias of 2 nA and 0.13 V, respectively of (a) PMNBT, (b) hDT, and (c) dDT on Au substrate; arrows in the upper left insets indicate spots where the currents were measured. Lower right insets show the histograms for the most frequently occurring current magnitude at 0.75 V. Average STM *I-V* curves (2nd order) for PMNBT (green), hDT (maroon), and dDT (blue) molecules along with bare gold are shown in (d).

3. Results and Discussions

The line spectra and the height measurements in the STM images were used to identify the bundle of the hDT, dDT, and PMNBT molecules (figure 2). The average heights of the individual peaks were ~2.0 nm and ~1.2 nm for hDT and dDT, respectively, representing the approximate size of the two molecules. The respective reported chain lengths with Au-thiol bonding are 1.8 nm and 1.4 nm (*18*). In case of the PMNBT SAM (figure 2c), the height of the individual spike was about 2.1 nm, representing the approximate length (2.16 nm) of the optimized PMNBT molecule (figure 1). The measured root mean square (rms) roughness for the 50×50 nm^2 scan area of the bare Au surface was 0.060±0.0041 nm, and that with adsorbed hDT and dDT were 0.048±0.02 nm and 0.058±0.014 nm, respectively. The almost identical roughness of the aforementioned three surfaces reflects the close-packed self-assembly of hDT and dDT with the formation of SAM. The PMNBT molecules, on the other hand, were less uniformly adsorbed on the surface and, thus, add to the measured surface roughness (rms = 0.17±0.011 nm). The difference in the density and uniformity of the SAM of the two molecules could be related to the difference in their chemical bonding and molecular structure. In the case of hDT and dDT, the molecular charge density has a small spatial extension due to σ-type bonding in the backbone, resulting in a rather short-range Coulomb field, thus allowing a denser packing of molecules. In contrast, the charge density in the π-conjugated backbone of PMNBT has large overall spatial extension below and above the molecular plane, creating greater intermolecular repulsion and steric hindrance, which leads to a less densely packed monolayer formation. It is worth noting that a greater intermolecular repulsion between π-electron conjugated systems may also induce conformational changes in adsorbed molecules, adding to the non-uniformity, and also to the electrical properties of the SAM.

The FTIR spectra of PMNBT, showing relative absorbance values, are provided in figure 3. In case of PMNBT, a reference spectrum of the PMNBT crystals is compared to spectrum of the SAM film. The amount of material probed in the case of the SAM film is significantly less, and the quality of the spectrum is not as good as for the crystals; nonetheless, the spectral features are comparable, indicating that the SAM deposition was successful. The bands between 2000–1600 cm^{-1} are indicative of the –C=N stretch and phenyl ring substitution overtones. The peaks above 3000 cm^{-1} are indicative of the C-H stretch of the aromatic ring of PMNBT. The FTIR spectra of many thiols have a unique band between 2550 cm^{-1} and 2600 cm^{-1}, which, although weak, is distinctly indicative of the S-H stretch. It is not always present, however, and unfortunately none of the compounds in this study exhibited it. Had it been present, it could potentially have been used to track the extent to which the SAMs are bonded to the Au, since the S-H bond break prior to Au-S bond formation. In the case of the hDT and dDT, the molecules consist primarily of C-C and C-H bonds, their FTIR spectra are dominated by these absorbances, and the S-H bands are not evident. For the case of aromatic thiols, we observed that nearly all of

the halogen-substituted aromatic thiols exhibited the S-H stretching mode, but that it was often not found in the amino-substituted compounds. Nonetheless, the FTIR did serve to confirm the presence of the SAM molecules on the Au substrate.

The tunnel current (*I*), as a function of applied tip bias (*V*), was measured at more than 10 spots (some of the spots are indicated by arrows in the upper left insets in figure 4) on each SAM sample. Each *I-V* trace was an average of 100 scans at any spot. The *I-V* curves for the PMNBT, hDT, and dDT SAMs are shown in figures 4a, 4b, and 4c, respectively. The measured tunnel current through the SAMs of σ-bonded molecules (hDT and dDT), as well as PMNBT molecules, exhibit a noticeable distribution in magnitude. However, the hDT and dDT SAMs show a much narrower spread in current magnitude than the PMNBT. The lower right insets in figures 4a, 4b, and 4c show the statistical distribution of the measured current values at +0.75 V, from which it is clear that the most frequently occurring current value for PMNBT is around 24 nA. The hDT and dDT SAMs exhibit a rather uniform distribution of measured tunnel current, with the most frequent tunnel current having a magnitude of ~0.005 nA for hDT and ~1.5 nA for dDT. The most frequently occurring current value in the hDT molecules is smaller by a factor of about two than that in the dDT molecules. Both hDT and dDT molecules are σ-bonded molecules and, hence, are expected to be virtually insulating molecules. However, the dDT molecules are smaller in length (~1.2 nm) compared to the hDT (~2.0 nm) molecules; the tunnel current is much smaller in hDT. On the other hand, the most frequently occurring tunnel current values for π-bonded PMNBT molecules are about three orders of magnitude higher than hDT molecules and one order of magnitude higher than dDT. The observation of large tunneling current via PMNBT compared to hDT and dDT is a consequence of the highly delocalized π-electron charge distribution in PMNBT molecules.

The values of transconductance, $g_o = (dI/dV)$, and corresponding quantum resistance, R_o, estimated from the measured *I-V* traces at an applied bias of 0.75 V are listed in table 1. Though g_o and R_o are generally measured at zero applied bias, we measured at the applied bias of +0.75 V. This was done to avoid the low signal-to-noise ratio regime of the STM (*18*). Our estimated value of g_o for dDT is about two orders of magnitude smaller than that reported earlier by Labonté et al (*18*) from a similar experiment but using an applied bias of –1.5 V. The difference in the value of g_o (and R_o) in the two measurements could be due to differences in experimental conditions, including different bias voltages, SAM preparation, and quality of the film, as well as the sensitivity of the STM. However, our measured g_o and R_o for dDT, which has been extensively studied, is within an order of magnitude of the literature values (*18*). It is noted that the value of g_o for the π-bonded molecule PMNBT is almost four orders of magnitude larger than σ-bonded hDT and almost two orders of magnitude larger than dDT molecules. A large magnitude of g_o for PMNBT makes it an attractive candidate for molecular-scale electronics applications.

Table 1. Estimated $g_0=(dI/dV)_{V=0.75}$ and corresponding resistance, R_0 of the molecules.

Substrate	**$(dI/dV)_{V=0.75}$ (S)**	**R_0 (Ω)**
hDT	$7.79\text{x}10^{-11}$	$1.66\text{x}10^{14}$
dDT	$7.15\text{x}10^{-9}$	$1.81\text{x}10^{12}$
PMNBT	$1.24\text{x}10^{-7}$	$1.04\text{x}10^{11}$

An interesting part of the measured tunnel currents in the molecular SAMs is the asymmetry with respect to the polarity of the bias voltage. The estimated distribution of the tunnel current with respect to the positive and negative bias voltages for the molecular SAMs, as well as the bare Au substrate, is listed in table 2. Asymmetric behavior in the *I–V* curves is observed for bare Au (11.0%), and the SAMs of hDT (24.9%) and dDT molecules (19.0%). In comparison, the PMNBT SAM molecule exhibits a significantly more pronounced asymmetry (40.6%) of the tunnel current. We also note that the *I-V* curves for the PMNBT molecules show three distinct behaviors (marked in figure 4a). Although, no specific reason is apparent, there could be several significant contributing factors. As indicated by the marked arrows in the upper-left inset of figure 4a, there are three different regimes where the *I-V* curves were measured which are differentiated by the brightness. The brightest spots, indicated by **1,** represent the maximum current, whereas the arrows marked **3** represent the lowest current. Moreover, the π-bonded PMNBT molecules have the tendency to change their geometrical conformation in response to external perturbation, leading to varying current magnitudes (*19*). Nonetheless, it is worth noting the prominent rectification in each region of current. This observed rectifying behavior in the case of PMNBT SAM can be seen more clearly in figure 4d, where the best second-order fit to the measured *I-V* curves for the SAMs of hDT (maroon), dDT (blue), and PMNBT (green) on the Au(111) substrate are plotted together. For reference, the corresponding *I-V* curve (yellow) for bare Au is also plotted. The magnitude of the current in the case of bare Au is much larger than those for the molecular SAMs.

Table 2. Average asymmetry in the current distribution observed in the three samples.

Gold	11.0%
hDT	24.9%
dDT	19.0%
PMNBT	40.6%

The observation of a large current rectification by PMNBT molecules, and not by hDT or dDT under similar experimental conditions, can be understood from the consideration of the physical and electronic structures of the STM probe-SAM-substrate system. Three possible factors can potentially contribute to the observed asymmetry in the measured tunnel current through PMNBT: (i) asymmetry due to a difference in the chemical nature (and chemical potential) of the substrate (Au) and the STM tip (Pt/Ir), (ii) difference in the electronic structure of the molecule-

substrate (Au) and molecule-STM tip interfaces, and (iii) electric-field induced change in conformation of the molecule. While the difference in the chemical nature of the substrate and STM tip will certainly have an effect due to different work functions of the metals, it alone cannot account for the observed asymmetry in the case of PMNBT. If this alone were the case, one would also observe similar behavior in hDT or dDT, especially since this molecule has a single –SH group and, hence, becomes somewhat asymmetric. The difference in the electronic structure and the charge distribution at the molecule-Au interface and at the molecule-Pt/Ir junction due to difference in chemical bonding at the two interfaces may induce D-A characteristics in the otherwise symmetric molecule, thus creating a medium for rectifying tunnel current. Indeed, the *ab initio* calculation (figure 1), which yielded an optimized Au-PMNBT-Au, suggests substantial charge (0.22e-) transfer from Au to sulfur (S) atoms. The charge at the S atom is mainly localized in the HOMO-1 level, which is a low-conjugated sp-type orbital with slight contributions from Au 4s shell. Thus, one would expect transfer of charge from Au to the S-end of the chemisorbed molecule, thus making the molecule electron rich (donor) at the Au-molecule interface. Since no bonds are formed at the STM side of the molecule, no effective charge transfer takes place, thus the molecule acquires an effective electron deficient (acceptor) characteristic at the molecule-air-Pt/Ir end. Due to this "induced" D-A characteristic of the molecule, the electrons will easily tunnel from the molecule to STM tip under positive tip-bias, but not vice versa, resulting in the observed rectification behavior. The ability of this charge to easily tunnel through the molecule, and to the Pt/Ir tip at positive bias, is facilitated by the highly delocalized nature of the HOMO (figure 1b), which is only 0.6 eV higher than the S atom containing the extra charge. A similar mechanism has also been proposed as a possible reason for the observed rectification in a previous experiment (*11*) on oligo (phenylethynyl) benzothiol and appears to be consistent with the present observation.

A conformational change of the conjugated-π electron system is known to affect its electrical transport properties. It has been shown on the basis of quantum mechanical calculations that a planar geometry, in which the π-orbitals in the molecule are parallel, gives a larger tunnel current (*19*) and electron transfer probability (*20*) through the molecule than a non-planar geometry. In order for the conformational change to cause rectification of tunnel current, one would expect that under a positive tip bias, the molecules (at least a great fraction of them) under the STM tip acquire an electrically favorable (planar) geometry, while the same is not true under reversed bias. The *ab initio* molecular orbital calculations do suggest that under equilibrium conditions, the molecule has a non-planar ground state geometry (figure 1c), with the middle diimino (-N=CH-C_6H_4-CH=N-) moiety rotated by ~33^o with respect to the molecular plane containing the two terminal phenyl rings. The difference in the total energy between the planar and the stable non-planar ground state geometry is calculated to be ~0.25 eV with HF and ~0.18 eV with density functional theory. Thus, it is possible that under applied bias, a number of molecules change their state from a non-planar to a planar geometry, therefore facilitating enhanced electron transport. More detailed experimental and theoretical investigations and analyses are required to exactly establish the underlying physical mechanism of the observed rectification.

However, the asymmetry due to charge transfer to the molecule at the Au-molecule interface appears to be the dominant mechanism, as also suggested by Dhirani et al. (*11*) in the case of oligo(phenylenacytelene)benzothiol.

4. Conclusions

In summary, we have performed STM measurements on electron tunneling characteristics of SAMs of a newly engineered π-conjugated molecule, PMNBT, together with the much studied σ-bonded, hDT, and dDT molecules. Both hDT and dDT molecules form close packed SAMs, as expected. PMNBT molecules also form somewhat patterned SAM. The PMNBT molecule exhibits a large tunneling current due to its highly conjugated π-electron structure. The PMNBT molecule also exhibits prominent rectification of the tunnel current, which appears to result from a combination of electronic and geometrical effects in the molecule and at the molecule-metal interface. In contrast, the tunneling current through the σ-bonded hDT and dDT SAMs has much smaller magnitude and exhibits very little asymmetry in the *I–V* curves. The PMNBT molecules, due to a large magnitude of tunnel current and rectifying property, may be useful for molecular-scale electronics applications.

5. References

1. Aviram, A.; Ratner, M. A Molecular Rectifiers. *Chem. Phys. Lett.* **1974**, *29*, 277–283.
2. Geddes, N. J.; Sambles, J. R.; Jarvis, D. J.; Parker, W. G.; Sandman, D. J. Fabrication and Investigation of Asymmetric Current-voltage Characteristics of Metal/Langmuir-Blodgett Monolayer/Metal Structure. *Appl. Phys. Lett.* **1990,** *56*, 1916–1918.
3. Martin, A. S.; Sambles, J. R.; Ashwell, G. J. Molecular Rectifier. *Phys. Rev. Lett.* **1993**, *70*, 218–221.
4. Fisher, C. M.; Burland, M.; Roth, S.; Klitzing, K. V. Organic Quantum Wells: Molecular Rectification and Single-electron Tunneling. *Europhys. Lett.* **1994**, *28*, 129–134.
5. Metzger, R. M.; Chen, B.; Hopfner, U.; Lakshmikantham, M. V.; Vuillame, D.; Kawai, T.; Wu, X.; Tachibana, H.; Hughes, T. V.; Sakurai, H.; Baldwin, J. W.; Hosch, C.; Cava, M. P.; Brehmer, L.; Ashwell, G. J. Unimolecular Electrical Rectification in Hexadecylquinolinium Tricyanoquinodimethanide. *J. Am. Chem. Soc.* **1997**, *119*, 10455–10466.
6. Metzger, R. M.; Chen, B.; Vuillame, D.; Laxmikantam, M. V.; Hopfner, U.; Kawai, T.; Baldwin, J. W.; Wu, X.; Tachibana, H.; Sakurai, H.; Cava, M. P. Observation of Unimolecular Electrical Rectification in Hexadecylquinolinium Tricyanoquinodimethanide. *Thin Solid Films* **1998**, *326*, 326–330.
7. Elbing, M.; Ochs, R.; Koentopp, M.; Fischer, M.; Hänisch, C. von.; Weigend, F.; Evers, F.; Weber, H. B.; Mayor, M. A Single-molecule Diode. *Proc. Natl. Acad. Sci.*, **2005**, *102*, 8815–8820.
8. He, H.; Pandey, R.; Mallick, G.; Karna, S. P. Asymmetric Currents in a Donor-Bridge-Acceptor Single Molecule: Revisit of the Aviram-ratner Diode. *J. Phys. Chem. C*, **2009**, *113*, 1575–1579.
9. Pomerantz, M.; Aviram, A.; McCorkle, R. A.; Li, L.; Schrott, A. G. Rectification of STM Current to Graphite Covered with Phthalocyanine Molecules. *Science*, **1992**, *255*, 1115–1118.
10. Stabel, A.; Herwig, P.; Mullen, K.; Rabe, J. P. Diode Like Current-voltage Curves for a Single Molecule-tunneling Spectroscopy with Submolecular Resolution of Alkylated Peri-condensed Hexabenzo Coronene. *Angew. Chem. Int. Ed. Engl.*, **1995**, *34*, 1609–1611.
11. Dhirani, A.; Lin, P.-H.; Guyot-Sinnoset, P.; Zehner, R. W.; Sita, L. R. Self-assembled Molecular Rectifiers. *J. Chem. Phys.*, **1997**, *106*, 5249–5253.

12. Kusmerick, J. G.; Holt, D. B.; Yang, J. C.; Naciri, J.; Moore, M. H.; Shashidhar, R. Metal-molecule Contacts and Charge Transport Across Monomolecular Layers: Measurement and Theory. *Phys. Rev. Lett.* **2002**, *89*, 086802 (1–4).

13. Mallick, G.; Griep, M, Lastella, S.; Sahoo, S.; Hirsch, S.; Ajayan P. M.; Karna, S. P. Diode-like Properties of As-grown Chemical Vapor Deposited Single-walled Carbon Nanotubes. *J of Nanosc. and Nanotech.* **2010**, *10*, 6062–6066.

14. Mallick, G.; Griep, M. H.; Ajayan P. M.; Karna, S. P. Alternating Current-to-Direct Current Power Conversion by Single-wall Carbon Nanotube Diodes. *Appl. Phys. Letts.* **2010**, *96*, 233109 (1–4).

15. Bumm, L. A.; Arnold, J. J.; Dunbar, T. D.; Allara, D. L.; Weiss, P. S. Electron Transfer through Organic Molecules. *J. Phys. Chem. B* **1999**, *103*, 8122–8127.

16. Wold, D. J.; Haag, R.; Rampi, M. A.; Frisbie, C. D. Distance Dependence of Electron Tunneling through Self-assembled Monoloayers Measured by Conducting Probe Atomic Force Microscopy: Unsaturated versus Saturated Molecular Junctions. *J. Phys. Chem. B* **2002**, *106*, 2813–2816.

17. Moutloali, R. M.; Nevondo, F. A.; Darkwa, J.; Iwuoha , E. I.; Henderson, W. Bimetallic Nickel Complexes with Bridging Dithiolated Schiff Base ligands: Synthesis Mass Spectral Characterization and Electrochemistry. *J. Organomet. Chem.* **2002**, *656*, 262–269.

18. Labonte, A. P.; Tripp, S. L.; Reifenberger, R.; Wei, A. Scanning Tunneling Spectroscopy of Insulating Self-assembled Monolayers on Au(111). *J. Phys. Chem. B* **2002**, *106*, 8721–8725.

19. Pati, R.; Karna, S. P. Current Switching by Conformational Change in a $\pi-\sigma-\pi$ Molecular Wire. *Phys. Rev. B* **2004**, *69*, 155419 (1–5).

20. Pati, R.; Karna, S. P. *Ab Initio* Hartree-Fock Study of Electron Transfer in Organic Molecules. *J. Chem. Phys.* **2001**, *115*, 1703–1715.

List of Symbols, Abbreviations, and Acronyms

Ag	silver
ARL	U.S. Army Research Laboratory
Au	gold
cAFM	conducting atomic force microscopy
CVD	chemical vapor deposited
DARPA	Defense Advanced Research Projects Agency
dDT	dodecanethiol
DRI	Directors's Research Initiative
ECP	effective core potential
ET	electron transport
FTIR	Fourier Transform Infrared
hDT	hexadecanethiol
HF	Hartree-Fock
HOMO	highest occupied molecular orbital
Ir	iridium
LUMO	lowest unoccupied molebular orbital
PMNBT	,4'-[1,4-phenylenebis(methylidynenitrilo)]bisbenzenethiol
Pt	platinum
S	sulfur
SAM	self-assembled monolayer
STM	scanning tunneling microscopy
SWCNTs	single wall carbon nanotubes
THF	tetrahydrofuran

NO. OF COPIES	ORGANIZATION
1 ELEC	ADMNSTR DEFNS TECHL INFO CTR ATTN DTIC OCP 8725 JOHN J KINGMAN RD STE 0944 FT BELVOIR VA 22060-6218
1 CD	OFC OF THE SECY OF DEFNS ATTN ODDRE (R&AT) THE PENTAGON WASHINGTON DC 20301-3080
1	US ARMY RSRCH DEV AND ENGRG CMND ARMAMENT RSRCH DEV & ENGRG CTR ARMAMENT ENGRG & TECHNLGY CTR ATTN AMSRD AAR AEF T J MATTS BLDG 305 ABERDEEN PROVING GROUND MD 21005-5001
1	US ARMY INFO SYS ENGRG CMND ATTN AMSEL IE TD A RIVERA FT HUACHUCA AZ 85613-5300
1	COMMANDER US ARMY RDECOM ATTN AMSRD AMR W C MCCORKLE 5400 FOWLER RD REDSTONE ARSENAL AL 35898-5000
1	NASA GLENN ATTN RDRL VT M VALCO 21000 BROOKPARK ROAD MAIL STOP 21-2 CLEVELAND, OH 44139-3191
1	US GOVERNMENT PRINT OFF DEPOSITORY RECEIVING SECTION ATTN MAIL STOP IDAD J TATE 732 NORTH CAPITOL ST NW WASHINGTON DC 20402

NO. OF COPIES	ORGANIZATION
1	US ARMY RSRCH LAB VTD-ODIR ATTN RDRL VT BLDG 4603 ABERDEEN PROVING GROUND, MD 21005-5069
31	US ARMY RSRCH LAB ATTN RDRL VT G MALLICK (10 HCS) ATTN RDRL WM (A) ATTN RDRL WM S KARNA (10 HCS) ATTN RDRL WML B P KASTE (10 HCS) BLDG 4600 ABERDEEN PROVING GROUND MD 21005
3	US ARMY RSRCH LAB ATTN IMNE ALC HRR MAIL & RECORDS MGMT ATTN RDRL CIO LL TECHL LIB ATTN RDRL CIO MT TECHL PUB ADELPHI MD 20783-1197

TOTAL: 42 (1 ELEC, 1 CD, 40 HCS)

INTENTIONALLY LEFT BLANK.